Proceedings of the 21st ICSMGE, Vienna, Austria, 14 – 19 June 2026. Pistrol, Adam & Schweiger (eds.)
Published by: ÖGG, Austrian Society for Geomechanics, Salzburg, Austria, ISBN 978-3-9503898-4-5
https://doi.org/10.53243/ICSMGE2026-1526

Experimental analysis of key factors governing effective thermal conductivity of granular media

Marina S Bortolotto
Department of Engineering, University of Cambridge, Cambridge, UK, ms3077@cam.ac.uk

David M G Taborda, Catherine O'Sullivan
Department of Civil and Environmental Engineering, Imperial College London, London, UK

ABSTRACT: Geomaterials are constantly subjected to thermal loads, which are caused by a variety of phenomena, including interaction with the atmosphere, buried cables and pipelines, and the operation of ground-source energy systems. Heat transfer within geomaterials is mainly governed by conduction. The capability of a media to conduct heat is quantified through the assessment of its thermal conductivity, which is influenced by many factors. Three main groups of factors affect the effective thermal conductivity of granular materials: particle contact, type and relative amount of pore fluid, and mineralogy. Particle contact is a broad concept that depends upon particle size, gradation (including fines content), angularity, density, and external pressure. Although there are studies investigating individual parameters, systematic studies investigating the impact of all individual factors are scarce. This contribution includes an overview of key parameters controlling the effective thermal conductivity and their significance. A new experimental dataset obtained through the use of needle probes, which are interpreted as a transient infinite-line heat source, is presented. The effect of particle contact was assessed in terms of porosity, gradation, particle size and shape. The effect of adding purified water to the pore spaces and the type of geomaterials were also assessed. The generated dataset was clearly clustered into four groups with increasing thermal conductivity: dry glass beads, dry natural sands, flushed glass beads, and flushed natural sands. Such natural clustering emphasises the dominance of the type of geomaterials and pore fluid on the effective thermal conductivity. These findings not only contribute to the fundamental understanding of thermal conductivity in porous media, but also provide more reliable parameters for simulating the thermal behaviour of the ground, leading to better design of geothermal heating/cooling systems and high voltage cabling.

KEYWORDS: Effective thermal conductivity, granular soils, thermal behaviour, needle probes, ground source energy.

1 INTRODUCTION

From a general perspective, there are three main mechanisms of heat transfer in materials: conduction, convection, and radiation (Çengel & Ghajar, 2015). Heat transfer within geomaterials is mainly governed by conduction (Farouki, 1981) when there is no water flow, and the capability of a media to conduct heat is quantified by its thermal conductivity, which is influenced by many factors.

The main factors affecting the thermal conductivity of porous media include the mineralogy, dry density (or porosity), pore size, gradation, the "quality of contacts" among particles, water content, temperature, and the type of fluid filling the pores (Bird et al. 2001; Mitchell & Soga, 2005; Santamarina & Park, 2016).

Prior observations indicate that the relative impact on each of these parameters on the thermal conductivity of granular soils differs. This means that an appropriate model to predict thermal conductivity needs to quantify the effect of each governing parameter.

It can be challenging to determine the thermal conductivity of a non-homogeneous or a porous medium as both the physical characteristics (e.g. thermal conductivity of different phases) as well as the volume and spatial distribution of each phase affect the overall conduction (Farouki, 1981). Abbasy (2009) and Atalay (2019) present a comprehensive and detailed description of the dependency of thermal conductivity on individual factors by presenting and discussing different predictive models.

There are many models available to predict the effective thermal conductivity of porous media ($k_{T,eff}$): from theoretical models, that establish upper and lower bounds, to empirical and semi-empirical models. The most relevant empirical and semi-empirical models for dry-granular-unfrozen soils (k_{dry}) include the following parameters: indication of dry density, particle shape parameters, and empirical parameters depending on the type of soil (i.e. fine sands) that typically need calibration. For saturated-unfrozen soils (k_{sat}), the parameters are: quartz content, thermal conductivity of quartz and other minerals composing the soil, thermal conductivity of water (or pore fluid), porosity, and degree of saturation. Some models also include empirical parameters depending on the type of soil or "texture" and shape factor. The value of $k_{T,eff}$ is usually a combination of k_{dry}, k_{sat}, and a variety of factors that usually require calibration – Bortolotto (2024) provides further details. Empirical and semi-empirical models often rely on calibration of the investigated soil, which means that the expansion of experimental datasets is of great importance.

A better fundamental understanding of individual factors contributing to the value of $k_{T,eff}$ of granular media is essential to develop more models to predict and describe the thermal behaviour of the ground. Improved predictive models will lead to better design and performance of geothermal heating/cooling systems and high voltage cabling, for instance. This study systematically investigates the impact of key governing factors on $k_{T,eff}$ of a variety of geomaterials with different physical characteristics and packed at a range of densities. Specimens were tested under dry and flushed (i.e. near to saturation) states. The experimental dataset was obtained using needle probes.

2 GOVERNING FACTORS OF $k_{T,eff}$

Bortolotto (2024) collated data from the literature that included 17 high-quality studies and 699 thermal conductivity measurements obtained from laboratory tests. From this dataset, it is evident that there are three main factors governing thermal conductivity of granular media: particle contact, pore fluid, and mineralogy.

Since conduction takes place through adjacent particles, the number and quality of contacts influence heat transfer. The nature and density of particle contacts depends upon a broad range of parameters, these include: particle size, gradation and (including fines content), particle shape, packing density or

porosity, and applied external pressure. In general, whenever changes in one or more of these parameters cause an increase in contact area or an increase in the number of contacts between particles (e.g. improved gradation), the $k_{T,eff}$ increases.

A second governing factor is the type of pore fluid and the percentage of voids occupied by it. Since water has a thermal conductivity, $k_{T,w}$ = 0.60 W/(m·K), 25 times larger than that of air, $k_{T,a}$ = 0.024 W/(m·K), varying the degree of saturation can drastically change the effective thermal conductivity (Mitchell & Soga, 2005).

The final parameter governing $k_{T,eff}$ is mineralogy. It is very clear that mineralogy and the respective solid thermal conductivity ($k_{T,s}$) plays a major role. This is generally accepted since the most accurate empirical and semi-empirical models include $k_{T,s}$ explicitly. In general, materials including particles with higher thermal conductivity present higher values of $k_{T,eff}$ for the same porosity.

3 NEEDLE PROBES: TRANSIENT INFINITE-LINE HEAT SOURCE

Thermal conductivity can be measured through either steady-state or transient methods (Farouki, 1981). Steady-state methods are more time consuming since they require a steady state heat flux to be achieved so that Fourier's law can be used to interpret the results. Transient methods are quicker and interpret the rate at which temperature changes over time using the transient form of the diffusion equation (Loveridge et al. 2017).

Transient methods rely on the diffusion of heat (Presley & Christensen, 1997; Loveridge et al. 2017). Four main transient methods can be applied to soils (Farouki, 1981; Presley & Christensen, 1997): thermal probes (needles), differentiated line-heat sources (dual needles), transient hot wires, and the thermal shock method.

The most common transient method is the thermal needle probe. The needle is slender enough (large length/diameter ratio) to be idealised (without substantial error) as an infinitely-long and thin heating element with zero heat capacity. Heating and temperature monitoring elements are encased in the probe as the applied power must be known and the temperature over time must be recorded once the needle probe is inserted into the soil specimen. In general, the data for the temperature variation over time are compared to an idealised equation for infinitely long and thin heating elements (ASTM, 2022) which can be inverted to yield the thermal conductivity of the material.

The differentiated line-heat source method is referred to here as the dual needle or dual-needle method for simplicity. This method is similar to the (single) needle method, although the heating element and the thermistor are positioned into two parallel needles separated by a few millimetres (Gawecka, 2017). Data interpretation strongly relies on knowing the distance between the two needles, as it is needed, together with the time taken for the heat pulse to travel between the heat source and the thermistor, for the determination of thermal diffusivity. The distance between needles can be unintentionally altered during their installation, especially while testing stiff soils (Martinez-Calonge, 2017).

3.1 *TEMPOS Thermal Properties Analyser*

The TEMPOS Thermal Properties Analyser is a standalone module manufactured by the METER Group (Figure 1) and it was used to obtain the $k_{T,eff}$ of granular geomaterials in the current study. This device employs a transient method that, through different sensors (needle or dual-needle), can obtain different thermal properties, including: thermal conductivity, resistivity, heat capacity, and diffusivity. This study is limited to thermal conductivity.

The TR-3 is a long single needle and represents the best design for soils (from dry to moist state), rock, concrete, and other solids and porous media (METER, 2018). The SH-3 is a dual-needle probe that can only be used in soils at the lower end of the thermal conductivity spectrum due to its upper measuring limit of 2 W/(m·K). The resolution of either needle is not explicitly stated by the manufacturer. Assuming that the resolution is the "smallest measurable unit" (Lade, 2016), thermal conductivity cannot be resolved better than 0.1 and 0.02 W/(m·K) for TR-3 and SH-3 sensors, respectively. The two probes were used to measure $k_{T,eff}$ in the current study.

The theory and equations of how to interpret the raw data using a theoretical infinite-line heat source can be found elsewhere (Bortolotto, 2024; Gawecka, 2017; Martinez-Calonge, 2017), TEMPOS provides thermal conductivity values and these values are presented in the current work.

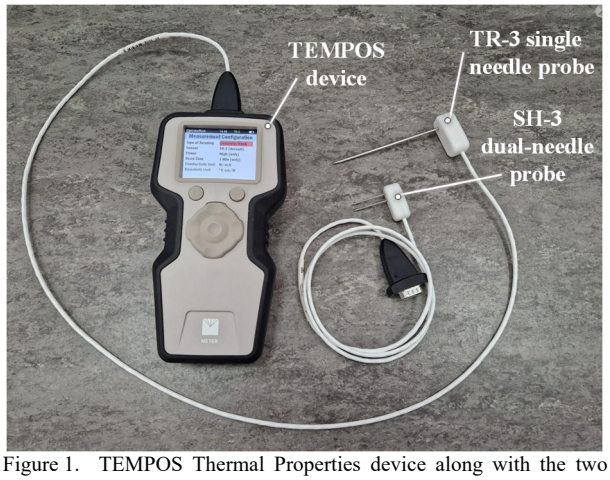

Figure 1. TEMPOS Thermal Properties device along with the two needle probes.

4 EXPERIMENTAL PROGRAMME

Five natural sands, five Soda Lime glass bead gradations ('SodaL_GB'), two Aluminium Borosilicate glass bead gradations ('AlBor_GB'), as well as an artificial geomaterial matching the particle size distribution (PSD) of Hostun sand comprising Soda Lime glass beads ('HS_SodaL_GB') were tested. Table 1 summarises the main physical features of the materials. Only granular materials were investigated, with only three of the tested materials (Sheffield, Osorio, and Dog's Bay sands) containing fines (<75 μm), limited to 0.2% in mass. The specific gravity of the various geomaterials varies from 2.51 to 2.70.

Data for three particle shape descriptors (Altuhafi et al. 2012) are also presented in Table 1: sphericity ($S_{x,50}$), aspect ratio (AR_{50}), and convexity ($C_{x,50}$). They were obtained through the dynamic image analyser module QICPIC, from Sympatec GmbH. These parameters contribute to advance the understanding of the effect of particle shape on $k_{T,eff}$. Furthermore, Table 1 includes classical descriptors of soils: coefficient of uniformity ($C_u = d_{60}/d_{10}$), coefficient of curvature ($C_c = (d_{30})^2/(d_{10} \cdot d_{60})$), d_{10} and d_{50}, which correspond to the diameter of particles at which 10% and 50% of the soil weight is finer, respectively – d_{30} and d_{60} can be interpreted in a similar way.

Table 2 presents values for solid thermal conductivity ($k_{T,s}$) for each geomaterial. The values were obtained based on the proportion of chemical composition of their mineralogy, further details can be found in Bortolotto (2024).

Table 1. Summary of investigated materials and their physical parameters.

Parameters	Sands					Glass beads							
							Soda Lime					Al. Borosilicate	
	Hostun	Sheffield	Osorio	Toyoura	Dog's Bay	Hostun Soda Lime glass beads	0.09 - 0.15 mm	0.15 - 0.25 mm	0.25 - 0.50 mm	0.50 - 0.75 mm	0.75 - 1.00 mm	0.50 - 0.80 mm	1.00 - 1.40 mm
C_u	1.69	1.76	1.52	1.32	1.70	1.69	1.40	1.21	1.16	1.12	1.11	1.17	1.19
C_c	1.02	1.03	0.93	1.00	0.91	1.10	1.07	1.02	0.99	1.00	1.01	0.99	0.97
d_{10} (μm)	234	154	127	179	138	233	102	211	336	643	852	610	1,038
d_{50} (μm)	366	248	177	226	198	370	138	247	379	710	928	693	1,191
Particle range (μm)	800 - 75	750 - <75	425 - <75	425 - 75	525 - <75	750 – 90	325 - <75	550 - 75	700 - 100	850 - 350	1,150 - 475	900 - 400	1,500 - 750
$S_{x,50}$	0.87	0.89	0.90	0.89	0.87	0.94	0.93	0.93	0.94	0.95	0.94	0.95	0.94
AR_{50}	0.73	0.75	0.76	0.75	0.69	0.94	0.87	0.86	0.95	0.96	0.97	0.97	0.98
$C_{x,50}$	0.93	0.93	0.93	0.93	0.92	0.96	0.93	0.94	0.96	0.98	0.98	0.98	0.99

Different ranges of glass beads sizes were used in the study as indicated in Table 1, e.g. 1.00 - 1.40 mm. While glass beads are expected to provide a more fundamental understanding of the thermal behaviour of perfect spheres (and respective contacts and pores), the testing of sands provides insight into the behaviour of typical natural granular materials.

Cylinders with a nominal length of approximately 162 mm and an internal diameter of 101 mm made of Perspex and PVC were used to contain the specimens (Figure 2). A total of 37 specimens were reconstituted either by funnel deposition or air pluviation. Dry specimens were densified by tapping on the side of the container, with up to five different densities being investigated. Fourteen out of the 37 dry specimens were flushed with water after reaching the target density.

For each specimen at a specific density and degree of saturation, four to six thermal conductivity measurements were performed at the top of the specimen, resulting in 564 measurements of $k_{T,eff}$. Needles were always pushed into the specimen (i.e. there was no pre-drilling). The position of needles on the surface of specimens is presented in Figure 2. The TR-3 single needle was positioned at the centre of the specimen and at three extra points equally spaced circumferentially, at a distance of 25 mm from the centre. The SH-3 dual needle was positioned at the centre only. While the finite dimension of specimens is a potential source of errors for needle tests (Presley & Christensen, 1997), boundary analyses were performed (Bortolotto, 2024) and considered unimportant for the current work. Tests were performed at room temperature (21 ± 1 °C) on a laboratory bench; no confinement or extra vertical load was imposed to specimens.

Table 2. Solid thermal conductivity coefficients ($k_{T,s}$) for the studied geomaterials.

Geomaterial		$k_{T,s}$ (W/(m·K))
Sand	Hostun	7.70
	Sheffield	3.92
	Osorio	7.70
	Toyoura	5.77
	Dog's Bay	3.85
Glass beads	Soda lime	1.13
	Aluminium-Borosilicate	1.13

Flushed specimens were achieved by flushing them with purified (through reversed osmosis) water from bottom to the top of the specimens. A small hydraulic gradient was used to avoid, as much as possible, disturbing particle arrangements and small particles' migration. By following this procedure, it is possible to claim that flushed specimens have virtually the same fabric as dry specimens, allowing a direct comparison of both states. Degrees of saturation ranging between 83% and 100% were achieved through this method.

The term 'flushed specimens' is preferred over 'saturated specimens' since some of the specimens did not reach full saturation (S_r=100%), therefore, strictly speaking, they are not saturated specimens. Even though the specimens are described as flushed, all the flushed specimens are within the so-called capillary regime (Lu & Dong, 2015), in which remaining air in the pores takes the form of occluded bubbles. This leads to a small increase in thermal conductivity for any additional amount of water since the porewater network is already existent.

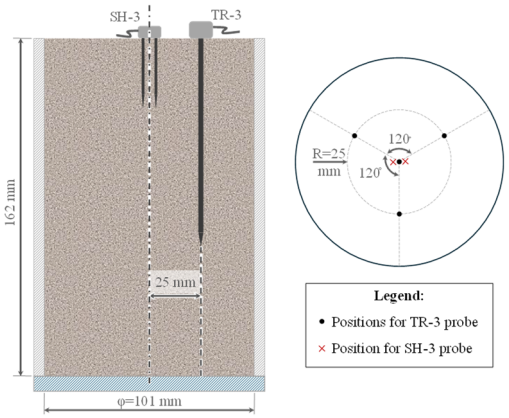

Figure 2. Schematic representation of tested specimens and needle probes (left-hand side); note that tests with different needles were not performed simultaneously. The position of needles on the circular surface is indicated on the right-hand side.

5 RESULTS

The new dataset is presented in Figure 3, in which $k_{T,eff}$ data are presented against specimen porosities. The dataset is naturally clustered into four groups (listed in order of increasing $k_{T,eff}$): dry glass beads, dry sands, flushed glass beads, and flushed sands. The porosity ranges obtained were 32-63% for the dry specimens and 36-47% for the flushed specimens.

5.1 *Repeatability and dispersion*

Statistical dispersion analysis indicated that the relative differences between individual measurements and the

respective average ($\bar{k}_{T,eff}$) are not significant for dry specimens. A maximum coefficient of variation (CV = sample standard deviation/$\bar{k}_{T,eff}$) among the entire dry dataset (CV = 11%) was obtained for Sheffield sand and 0.50-0.75 mm Soda Lime glass beads. These CV values agreed well with CV values given in the literature and the expected precision range for needle tests determined by ASTM D5334- 22a$^{\varepsilon 1}$ (ASTM, 2022). CV data for the flushed specimens differed, with a maximum CV value of 27% being encountered for Toyoura sand. This level of dispersion was larger than that observed by Tarnawski et al. (2015), who also reported an increase in CV for higher degrees of saturation in sandy soils.

To evaluate the repeatability of the experiments, dry specimens with the same porosity (to the nearest 1%) had their average $k_{T,eff}$ compared. The adopted method seems to be within the reported variation of repeatability in the literature.

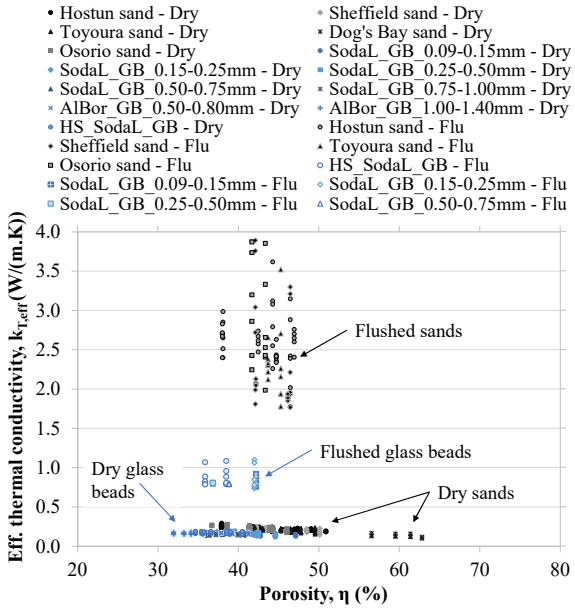

Figure 3. Dataset obtained through needle probe measurements naturally clustered into four (indicated) groups: sands and glass beads in dry and flushed (Flu) states.

5.2 *Effect of particle contact*

Although unclear in Figure 3, both the dry and flushed specimens demonstrated an overall clear increase in $k_{T,eff}$ as porosity decreases. Effects of porosity were more evident for dry specimens due to scatter in the dataset related to flushed samples. For clarity, the dry data are isolated in Figure 4, presenting average values of $k_{T,eff}$ for individual specimens. For dry sands, the increase in $k_{T,eff}$ with decreasing porosity is almost linear, in agreement with Lu et al. (2007) and Xiong et al. (2023).

Considering the data on Figure 4, the increase in $k_{T,eff}$ with decreasing porosity for dry glass beads is not only more subtle than for dry sands, but also, glass beads seem to switch to a much more gentle slope for porosities smaller than ~37%, so that the observed increase in $k_{T,eff}$ with decreasing porosity is small for porosities less than 37%.

The effect of particle size and gradation can be observed in Figure 4. There is a small increase in $k_{T,eff}$ with increasing diameter of the diameter of Soda Lime glass beads up to 0.50 mm. This is in agreement with findings that higher $k_{T,eff}$ is expected for larger particle sizes (Yun & Santamarina, 2008; Dong et al. 2015; Xiao et al. 2019). This mechanism can be explained by heat being transferred through only a fraction of the contacts; in other words, there is a preferential or critical path for transport phenomena (Sahimi & Tsotsis, 1997).

There is a degree of overlapping among the datasets for the Soda Lime glass beads with 0.25-0.50 mm and 0.50-0.75 mm gradations and Aluminum Borosilicate 0.50-0.80 mm. This perhaps characterises the limit in $k_{T,eff}$ gains due to increasing particle size. According to the Batchelor and O'Brien (1977) model, heat transfer through particle contacts relies on the harmonic mean between particles' diameters and other factors, which requires further work for conclusive analysis.

Even though HS_SodaL_GB has finer particles (d_{50} = 0.37 mm) than the two biggest size glass bead specimens (d_{50}~0.70 mm), this material is better graded than any other glass beads and this explains the overall higher values of $k_{T,eff}$ for HS_SodaL_GB. This potentially indicates a more significant impact of gradation on $k_{T,eff}$ in comparison to particle size.

HS_SodaL_GB was specially developed to evaluate the role of particle shape through comparisons with Hostun sand. Due to its less angular particles, however, HS_SodaL_GB porosities were mostly smaller than those of Hostun sand, resulting in only a limited overlap of porosities.

Dog's Bay sand reached the highest porosities among all investigated materials, which is explained by the high angularity of its particles. Therefore, it presents the lowest observed $k_{T,eff}$ values for dry sands. In other words, the number of contacts and the quality and area of these contacts are smaller, limiting heat conduction. Moreover, despite being disconnected from other dry sands, it is possible to include Dog's Bay sand measurements by extending the overall (roughly) linear relationship of $k_{T,eff}$ versus porosity for natural dry sands.

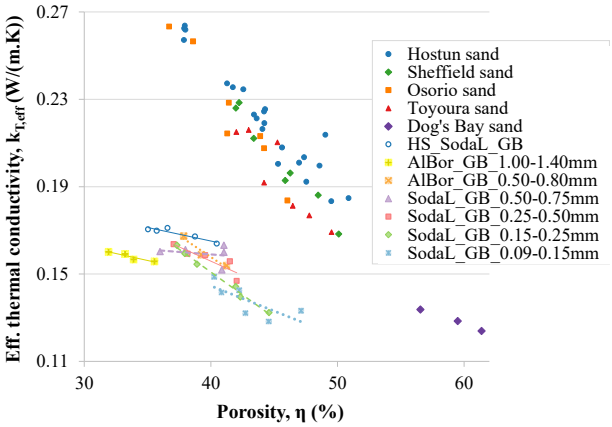

Figure 4. Average measurements of all dry specimens. Linear regressions for each type of glass beads are presented for better distinction between them.

Toyoura sand registered values of thermal conductivity close to the theoretical lower bound (series-flow model available in Farouki, 1981) of $k_{T,eff}$ values for dry sands with porosities between ~42% and 50%. These low values can be attributed to the fact that Toyoura sand is quite uniform, which leads to fewer particle contacts. For similar porosities, while Sheffield sand has a lower $k_{T,s}$ (as discussed in the following section), it presented an overall behaviour slightly above that of Toyoura sand, which is believed to occur due to better gradation, given that both sands have similar d_{50}. This means that Sheffield sand potentially has more contacts between particles than Toyoura sand.

Hostun sand presented the highest values of $k_{T,eff}$ among all natural sands. For lower porosities (<40%), only Hostun and Osorio sands are investigated (Figure 4). Osorio sand is finer

than Hostun sand and presents slightly lower values of $k_{T,eff}$, which highlights the effect of particle size since both sands have high quartz content and, therefore, have virtually the same $k_{T,s}$ (Table 2).

5.3 *Effect of mineralogy*

The data in Figure 4 may be influenced by mineralogy. Mineralogy impacts $k_{T,s}$ and so the $k_{T,eff}$. Data from Figure 4 are presented normalized by the relevant $k_{T,s}$ in Figure 5. Plotting the $k_{T,eff}$ data normalized by $k_{T,s}$ in Figure 5 allows the relative influences of changes in gradation and changes in mineralogy to be appreciated.

Hostun and Osorio sands both have a high quartz content and their normalised values (Figure 5) seem to cluster together in a relatively linear relationship with porosity. Their overlap, perhaps, indicate that despite Osorio sand (d_{50}=0.177 mm) being slightly finer than Hostun sand (d_{50}=0.366 mm), the difference in particle size is not enough to exhibit a clear difference between the two sands when normalised by $k_{T,s}$. This reinforces the dominating effect of $k_{T,s}$ in comparison with other factors influencing $k_{T,eff}$, such as particle size.

The Toyoura sand data are close to the lower bound of the sand $k_{T,eff}$ data on Figure 4; the data on Figure 5 indicate this may be explained in part by the lower quartz content (75%) of Toyoura sand. Toyoura sand presents slightly higher ratios ($k_{T,eff}$ /$k_{T,s}$) compared to Hostun and Osorio sands for the entire porosity range. Indicating that the differences in gradation (i.e. particle contact) have a larger influence on the relative values of $k_{T,eff}$ than the differences in $k_{T,s}$ or mineralogy. Similar trends are also observed for Sheffield sand and Dog's Bay sands.

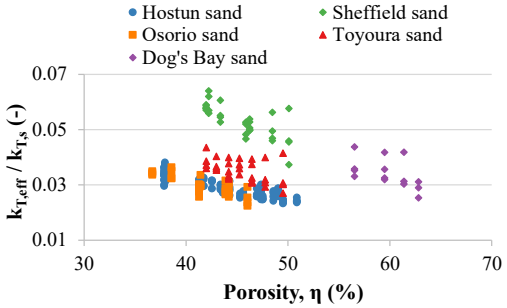

Figure 5. Effective thermal conductivity ($k_{T,eff}$) normalised by the respective thermal conductivity of solids ($k_{T,s}$) for dry natural sands.

Comparing the data for glass beads and the data for natural sands, it is clear that glass beads have lower values of $k_{T,eff}$ for similar porosities (Figure 4) and even for comparable degrees of saturation (Figure 3). This is expected since the $k_{T,s}$ of glass beads (1.13 W/(m·K)) is considerable smaller than that of any natural sands (3.85 - 7.70 W/(m·K)). In effect, Hostun sands' $k_{T,s}$ is 6.8 times bigger than that of Soda lime. However, the difference in $k_{T,s}$ cannot explain entirely the difference in $k_{T,eff}$ values since this value is only 3.8 times larger for Hostun sand. This difference highlights the impact of particle shape on $k_{T,eff}$.

5.4 *Effect of pore fluid*

The impact of saturation (or flushing) on $k_{T,eff}$ depends on the geomaterial. For similar porosities, while flushed sands have a $k_{T,eff}$ that is about 13 times that of the dry $k_{T,eff}$, the $k_{T,eff}$ for the flushed glass beads is only about 6 times the dry $k_{T,eff}$. Yun & Evans (2010) observed similar trends while saturating specimens, with gains in $k_{T,eff}$ of sands being 1.5 times larger than gains observed for glass beads. This effect of saturation is slightly lower than that measured in the current work (2.2 times), which only reinforces the complex mechanisms that occur within saturated media.

Hostun sand and its Soda Lime glass bead counterpart (HS_SodaL_GB) presented considerably different gains in $k_{T,eff}$ after flushing, despite the similarities in void ratio. The highest gain in $k_{T,eff}$ (after flushing specimens) was observed for Hostun sand, which coincidently presents a $k_{T,s}$ 6.8 times bigger than Soda Lime glass beads. Hence, the observed difference in gains for different materials suggests that water is indeed interconnecting pores (e.g. capillary regime) that are now filled with a 25 times more conductive fluid, which creates (higher conductivity) fluid paths connecting particles that were potentially not contributing as much when the sample was dry. Moreover, these results suggest that while water is a facilitator of heat transfer, a considerable amount of heat transfer is still occurring through solid particles. This highlights the role of the material, or, in the present case, the role of the thermal conductivity of the minerals ($k_{T,s}$) on heat transfer at high saturation levels.

Despite experimental evidence indicating that conduction through contacts is the predominant heat transfer mechanism in dry porous media (e.g. Yun & Santamarina, 2008), simulations from Cheng et al. (1999) indicate that conduction through stagnant fluid between particles in contact represents 64% and 80% of the total heat transfer for dry and moist specimens, respectively. Despite diverging from the current understanding of heat transfer, the simulations provide enlightening suggestions about the shift of the relative importance of different heat transfer mechanisms when switching the pore fluid. Therefore, the impact of these complex interactions can possibly explain different gains for different geomaterials once flushed with the same amount of water, as it is the case for Hostun sand and HS_SodaL_GB.

The current study used high-quality water (purified through reversed osmosis), which does not include ions in quantities close to those present in tap water or groundwater. In fact, the addition of salts (i.e. increase in salinity), for instance, decreases the thermal conductivity of water (Sharqawy, 2013). This means that the current study probably reflects the upper limit $k_{T,eff}$ achievable through saturation of similar soil specimens.

6 CONCLUSIONS

Thirteen granular geomaterials were investigated in the present work. Specimens were prepared with porosities ranging from 32-63% for dry specimens (S_r = 0%) and 36-47% for flushed specimens (83% ≤ S_r ≤ 100%). Measurements of $k_{T,eff}$ were obtained through needle probe tests (TEMPOS Thermal Properties Analyser), reaching repeatability and dispersion values expected for this method for dry specimens; flushed specimens presented a rather high dispersion.

In total, 564 measurements of $k_{T,eff}$ were performed and the obtained dataset is naturally clustered in four groups: dry glass beads, dry sands, flushed glass beads, and flushed sands – with $k_{T,eff}$ increasing from the former to the latter.

This natural arrangement of the dataset reinforces the effect of the key factors that are believed to govern $k_{T,eff}$ of granular geomaterials. The order of influence of these factors (from the current dataset) seems to be: pore fluid > mineralogy > particle contact. However, it should be noted that these are intertwined factors and establishing the individual effects of a complex phenomenon as heat transfer through porous media is challenging.

Water has a thermal conductivity 25 times larger than air, hence, the replacement of air by water leads to a gain in $k_{T,eff}$ that corresponds to the biggest gain in $k_{T,eff}$ among all governing factors. Different geomaterials are affected differently by the addition of water, with the sands, which are high in quartz content, being the geomaterials with the highest gain in $k_{T,eff}$ – up to 13 times when comparing dry and flushed states. It should be reminded, however, that the current study, and associated conclusions, is limited to the comparison of dry specimens to near fully saturated specimens.

The effect of particle contact was assessed in terms of porosity, gradation, particle size, and, potentially, particle shape. For the developed dataset, $k_{T,eff}$ seems to be more sensitive to gradation (C_u) than to particle size, which was evaluated in terms of d_{50}. While this is more evident for dry glass beads than for dry sands, it remains significant for both types of geomaterials. Further conclusions about particle shape are limited since this factor itself imposes a physical limit to the achievable porosities and, therefore, corresponds to a limitation of the dataset. The effect of porosity is undoubtfully significant for $k_{T,eff}$, in agreement with conclusions presented by Yun & Santamarina (2008), which suggested this as the most important macroscale parameter for $k_{T,eff}$ of dry soils.

Although it is recognised that isolating the effect of mineralogy is difficult, the fact that the group of sands consistently presents values of $k_{T,eff}$ greater than those for glass beads for both dry and flushed states is a great indication of its importance, particularly when sands also present the largest values of $k_{T,s}$. No other factor that corresponds to particle contact can justify the total differences in $k_{T,eff}$ between sands and glass beads, for the current dataset. Therefore, mineralogy is extremely important, but since conduction relies on contact, there is a deep and complex connection with other factors.

The current dataset and resulting conclusions contribute to the fundamental understanding of heat transfer in granular geomaterials and its underlying mechanisms. The high quality and reliable data generated also contributes to the existent dataset used for empirical models, which rely heavily on calibrations. Consequently, this study contributes to more accurate simulation of the thermal behaviour of the ground, leading to improved designs and performance of, for instance, geothermal heating/cooling systems or high voltage cabling.

7 ACKNOWLEDGEMENTS

This project was part of MATHEGRAM, a Marie SKŁODOWSKA-CURIE Innovative training network funded through the People Programme (Marie SKŁODOWSKA-CURIE Actions) of the European Union's Horizon 2020 Programme H2020 under REA grant agreement No. 813202.

8 REFERENCES

Abbasy, F. 2009. *Thermal Conductivity of Mine Backfill.* MSc Dissertation. Department of Building, Civil and Environmental Engineering, Concordia University.

Altuhafi, F., O'Sullivan, C., and Cavarretta, A.I. 2012. Analysis of an Image-Based Method to Quantify the Size and Shape of Sand Particles. *Journal of Geotechnical and Geoenvironmental Engineering*, 139 (8), 1290-1307.

ASTM, 2022. *ASTM D5334 - 22aε1 Standard Test Method for Determination of Thermal Conductivity of Soil and Rock by Thermal Needle Probe Procedure*. West Conshohocken, PA: ASTM International.

Atalay, F. 2019. *Engineered transition zone systems for enhanced heat transfer in thermo-active foundations*. PhD Thesis. School of Civil and Environmental Engineering, Georgia Institute of Technology.

Batchelor, G. K., and O'Brien, R. 1977. Thermal or electrical conduction through a granular material. *Proc. R. Soc. Lond.: A Math. Phys. Sci., 355 (1682): 313–333* .

Bird, R.B., Stewart, W.E., and Lightfoot, E.N. 2001. *Transport phenomena*. 2nd Edition. New York, NW: Chichester, J. Wiley.

Bortolotto, M.S. 2024. *Characterisation of the thermo-hydro-mechanical behaviour of granular materials*. PhD Thesis. Department of Civil and Environmental Engineering, Imperial College London.

Çengel, Y.A., and Ghajar, A.J. 2015. *Heat And Mass Transfer: Fundamentals & Applications*. 5th Edition. New York, NW: McGraw-Hill Education.

Cheng, G.J., Yu, A.B., and Zulli, P. 1999. Evaluation of effective thermal conductivity from the structure of a packed bed. *Chemical Engineering Science*, 54 (19), 4199–4209.

Dong, Y., McCartney, J.S., and Lu, N. 2015. Critical Review of Thermal Conductivity Models for Unsaturated Soils. *Geotechnical and Geological Engineering*, 33 (2), 207–221.

Farouki, O.T. 1981. *Thermal properties of soils*. CRREL Monograph 81-1. New Hampshire: U.S. Army Cold Regions Research and Engineering Laboratory Hanover.

Gawecka, K.A. 2017. *Numerical modelling of geothermal piles*. PhD Thesis. Department of Civil and Environmental Engineering, Imperial College London.

Lade, P.V. 2016. *Triaxial Testing of Soils.* Chichester, West Sussex: Wiley Blackwell.

Loveridge, F., Low, J., and Powrie, W. 2017. Site investigation for energy geostructures. *Quarterly Journal of Engineering Geology and Hydrogeology*, 50 (2), 158–168.

Lu, S., Ren, T., Gong, Y., and Horton, R. 2007. An Improved Model for Predicting Soil Thermal Conductivity from Water Content at Room Temperature. *Soil Science Society of America Journal*, 71 (1), 8–14.

Lu, N., and Dong, Y. 2015. Closed-Form Equation for Thermal Conductivity of Unsaturated Soils at Room Temperature. *Journal of Geotechnical and Geoenvironmental Engineering*, 141 (6), 04015016.

Martinez-Calonge, D. 2017. *Experimental Investigation of the Thermo-Mechanical Behaviour and Thermal Properties of London Clay*. PhD Thesis. Department of Civil and Environmental Engineering, Imperial College London.

METER. 2018. TEMPOS User Manual. Pullman, WA: METER Group.

Mitchell, J.K., and Soga, K. 2005. *Fundamentals of Soil Behavior*. 3rd Edition. New York: Wiley.

Presley, M.A., and Christensen, P.R. 1997. Thermal conductivity measurements of particulate materials1. A review. *Journal of Geophysical Research: Planets*, 102 (E3), 6535–6549.

Sahimi, M., and Tsotsis, T.T. 1997. Transient Diffusion and Conduction in Heterogeneous Media: Beyond the Classical Effective-Medium Approximation. *Industrial & Engineering Chemistry Research*, 36 (8), 3043–3052.

Santamarina, J.C., and Park, J. 2016. Geophysical properties of soils. In: B.M. Lehne, H.E. Acosta-Martinez, & R. Kelly (eds.). *Proceedings of the 5th International Conference on Geotechnical and Geophysical Site Characterisation*. Gold Coast, QLD, AU, 2016. Sydney, AU: Australian Geomechanics Society.

Sharqawy, M.H. 2013. New correlations for seawater and pure water thermal conductivity at different temperatures and salinities. *Desalination*, 313 (2013), 97-104.

Tarnawski, V.R., Momose, T., McCombie, M.L., and Leong, W.H. 2015. Canadian Field Soils III. Thermal-Conductivity Data and Modeling. *International Journal of Thermophysics*, 36 (1), 119–156.

Xiao, Y., Nan, B., and McCartney, J.S. 2019. Thermal Conductivity of Sand–Tire Shred Mixtures. *Journal of Geotechnical and Geoenvironmental Engineering*, 145 (11), 06019012.

Xiong, K., Feng, Y., Jin, H., Liang, S., Yu, K., Kuang, X., and Wan, L. 2023. A new model to predict soil thermal conductivity. *Scientific Reports*, 13 (1), 10684.

Yun, T.S., and Santamarina, J.C. 2008. Fundamental study of thermal conduction in dry soils. *Granular Matter*, 10 (3), 197–207.

Yun, T.S., and Evans, T.M. 2010. Three-dimensional random network model for thermal conductivity in particulate materials. *Computers and Geotechnics*, 37 (7), 991–998.